

Hybrid Offline–Online Signature Verification with Cross-Writer Mismatch Modelling and Fuzzy Fusion

Anjali Rohilla ¹ , Rajesh Kumar Bawa ²

¹ Department of Computer Science

Punjabi University

Patiala, India

e-mail: rohillaanjali.cs@gmail.com

² Department of Computer Science

Punjabi University

Patiala, India

e-mail: rajesh.k.bawa@gmail.com

Abstract

This paper presents a hybrid signature verification framework integrating offline handwritten signature images and online dynamic signing information for reliable biometric authentication. Offline signatures are represented using structural gradient-based descriptors, while online signatures are characterised through temporal and statistical features extracted from log trajectories. Both modalities are fused into a unified feature space, normalised, and reduced using principal component analysis for efficient learning. Writer-independent evaluation is performed using group-based cross-validation with cross-writer mismatch modelling to strengthen resistance against multimodal forgery attempts. Random

Received: 08 December 2025

Forest and Gradient Boosting classifiers are trained and combined through ensemble probability fusion, while fuzzy membership based decision support improves stability under uncertain verification conditions. Experimental results show competitive writer-independent accuracy with very low false rejection and equal error rates, confirming the effectiveness of multimodal fusion and fuzzy ensemble learning. The proposed framework provides a practical and robust solution for secure signature-based authentication systems.

Key Words and Phrases: Signature; Verification; Biometrics; Offline; Online; Fusion; Fuzzy; Ensemble; Authentication; Accuracy; FAR; FRR; EER.

1 Introduction

Handwritten signature verification remains one of the most widely accepted biometric authentication techniques because it is socially trusted, legally recognized, and easy to deploy in daily financial and administrative processes. Unlike physiological biometrics, signatures represent a behavioral trait that naturally varies with time, writing conditions, and the signer's physical state. These variations make the verification task challenging, particularly in writer-independent settings where the system must generalize to unseen users and skilled forgeries.

Recent progress in offline handwritten signature verification has been strongly influenced by deep learning architectures that aim to learn discriminative representations directly from signature images. Li *et al.* proposed a multi-scale CNN-CrossViT network that integrates convolutional feature extraction with transformer-based cross-attention to capture both local stroke patterns and global structural dependencies, achieving strong performance on public datasets [1]. Similarly, Xiao and Wu introduced a spatial transformer network framework to improve robustness against geometric

distortions by aligning signatures before feature learning [2]. These studies highlight the importance of multi-scale representation and spatial normalization for reliable verification.

Beyond signature verification, related research in writer identification has shown that robust feature modeling remains central for discriminating writing styles under constrained training conditions. Khan *et al.* presented bagged discrete cosine transform features for text-dependent writer identification, showing that ensemble-based representations can improve robustness [3]. Optimization strategies have also been explored for learning under complex constraints. Wei *et al.* proposed a coevolutionary neural-based optimization algorithm for constrained nonconvex problems, providing insights into improving learning stability in difficult biometric scenarios [4]. Adversarial learning has further contributed to signature verification, where Li *et al.* introduced an adversarial variation network to enhance generalization under intra-class variability [5].

Several end-to-end deep architectures have been developed for offline verification. Lu *et al.* proposed a cut-and-compare network that performs verification through structured comparison of signature regions [6]. Jain *et al.* showed that even shallow convolutional networks can provide competitive baselines when trained with suitable feature representations [7]. Deep learning improvements in other imaging domains, such as cascaded fully convolutional networks with variable focal loss, also motivate the design of robust loss functions for handling imbalance and difficult samples [8]. High-dimensional representation learning has been extended through tensor-based approaches such as NeuLFT, which addresses incomplete data modeling in complex feature spaces [9].

Traditional handcrafted approaches remain relevant as they provide interpretable structural cues. Zois *et al.* proposed poset-oriented grid features for offline verification and quality characterization [10]. Bharathi and Shekar employed chain code histograms with support vector machines, illustrating the effectiveness of directional contour descriptors [11]. Graph-based learning has also been explored, where Maergner *et al.* combined graph edit distance with

triplet networks to improve verification performance [12]. These works indicate that hybrid strategies combining learned and structural features can strengthen robustness.

Feature selection and streaming feature modeling have also been investigated. Wu *et al.* proposed latent factor analysis for online sparse streaming feature selection, which is relevant for dynamic biometric systems [13]. Fuzzy similarity modeling has been applied by Alaei *et al.*, who developed an interval symbolic representation with fuzzy similarity measures to handle uncertainty in signature traits [14]. Optimization-enhanced latent factor methods have further contributed to stable representation learning, as shown by Luo *et al.* through generalized Nesterov acceleration in adaptive latent factor analysis [15].

Multi-task learning has emerged as a useful paradigm in signature-related biometrics. Jain *et al.* showed multi-task learning using GNet features with SVM classifiers for signature identification [16]. Matrix factorization approaches with symmetry and nonnegativity constraints have also supported community detection and structured representation learning, offering transferable concepts for biometric clustering [17]. Sharif *et al.* emphasized best feature selection strategies for offline verification frameworks, reinforcing the importance of discriminative feature pruning [18]. Geometric feature design has been further explored by Khan *et al.*, who proposed novel geometric descriptors for offline writer identification [19]. Texture-based fusion strategies have been investigated by Bhunia *et al.*, where hybrid texture feature fusion improved verification accuracy [20].

Recent advances increasingly focus on generalizable deep representations. Luo *et al.* proposed pointwise mutual information incorporated symmetric nonnegative matrix factorization for accurate structure discovery, which supports robust feature modeling in high-dimensional biometric spaces [21]. Earlier writer-independent verification methods such as surroundedness feature extraction showed that local shape context remains important for distinguishing genuine and forged signatures [22]. Synthetic signa-

ture generation combined with Siamese neural networks has been proposed by Ruiz *et al.*, showing that compositional augmentation can reduce data scarcity [23]. Comparative evaluations of feature descriptors such as SURF and SIFT further motivate careful selection of discriminative local representations [24]. Hu and Chen showd that classifier combinations, such as AdaBoost over pseudo-dynamic features, can improve offline verification performance [25]. Finally, Jain *et al.* confirmed that geometric feature modeling with neural classifiers remains a competitive baseline for signature verification [26].

Overall, the literature indicates that signature verification requires robust multi-scale representation, strong generalization under writer-independent constraints, and effective fusion of complementary information sources. Motivated by these findings, the present work develops a hybrid signature verification framework that integrates offline image-based descriptors with online dynamic traits, supported by machine learning classification and fuzzy decision-level fusion to improve reliability against skilled forgeries.

1.1 Contributions of this work

- i. A hybrid offline–online signature verification framework is implemented by fusing static image descriptors with dynamic behavioural log features.
- ii. Cross-writer mismatch modelling is incorporated to strengthen security against multimodal forgery attempts under writer-independent conditions.
- iii. An ensemble learning strategy combining Random Forest and Gradient Boosting is developed to improve discrimination between genuine and forged signatures.
- iv. A fuzzy membership based decision fusion mechanism is introduced to handle uncertainty in borderline verification cases and reduce abrupt thresholding errors.

- v. Extensive evaluation using FAR, FRR, EER, ROC-AUC, and aggregated cross-validation confirms competitive writer-independent verification performance.

2 Implemented Hybrid Signature Verification Framework

This research implements a hybrid signature verification framework that integrates both offline and online signature modalities into a unified machine learning based authentication system. The offline modality represents the static visual appearance of a handwritten signature captured as an image, whereas the online modality represents the dynamic behavioural information recorded during the signing process, such as pen trajectory, time variation, and pressure signals. The motivation behind using both modalities is that skilled forgeries may imitate the visual shape of a signature, but replicating the underlying writing dynamics remains significantly more difficult. Therefore, combining offline and online evidence improves robustness and reliability in biometric verification.

Let a signature sample be represented by the pair

$$S = (I, L), \quad (1)$$

where I denotes the offline signature image and L denotes the online log file containing temporal and dynamic measurements. The objective of the system is to determine whether the given signature belongs to a genuine writer or represents a forged or mismatched instance.

The verification task is formulated as a binary classification problem. Each sample is associated with a label

$$y \in \{0, 1\}, \quad (2)$$

where $y = 0$ indicates a genuine and consistent signature pair, and $y = 1$ indicates a forged or inconsistent signature.

The complete implemented framework consists of five major stages: dataset collection, preprocessing, feature extraction, hybrid feature fusion with dimensionality reduction, and classification with fuzzy decision support. The final deployed system provides both writer-independent generalisation and robust security against cross-writer modality mismatches.

2.1 Dataset Description

The experiments in this work are conducted on a multimodal signature dataset collected from more than 120 writers. For each writer, two complementary modalities are recorded: offline handwritten signature images and online dynamic writing logs. The dataset is organised in a writer-wise folder structure, where each writer directory contains two subfolders: an *Image* folder and a *Log* folder.

The *Image* folder contains offline signature images captured using an Android-based acquisition application rather than conventional scanning. This acquisition setting introduces realistic variations in background, illumination, and writing surface conditions. The *Log* folder contains online signature trace files stored in `.txt` format, generated during signing on a mobile device or digital writing pad.

Each online log file records the real-time pen-tip trajectory using six parameters:

$$\text{TouchEvent Time} \mid X \mid Y \mid \text{raw}X \mid \text{raw}Y \mid \text{Pressure.} \quad (3)$$

These signals capture temporal progression, spatial movement, stroke direction, and pressure variation throughout the signing process. Such behavioural characteristics are highly writer-specific and difficult to reproduce accurately in skilled forgery attempts.

By combining offline image-based features representing signature shape and texture with online dynamic features representing speed, timing, movement continuity, and pressure, the proposed

system learns both the global visual appearance and the underlying neuromotor behaviour of the signer. This multimodal dataset configuration reflects practical verification environments in banks, offices, and institutional authentication settings, where signatures may be acquired either on paper (offline) or through digital devices (online).

2.2 Offline Signature Processing and Feature Extraction

The offline component of the system focuses on extracting discriminative structural and texture information from signature images. Each signature image is first converted into grayscale and resized to a fixed spatial resolution of 256×256 pixels. This standardisation ensures consistent feature dimensionality across all samples.

Let the grayscale signature image be denoted as

$$I_g(x, y), \quad (4)$$

where (x, y) represents pixel coordinates. The image is normalised to the range $[0, 1]$ as

$$I_n(x, y) = \frac{I_g(x, y)}{255}. \quad (5)$$

To represent the offline signature effectively, Histogram of Oriented Gradients (HOG) descriptors are employed. HOG captures local gradient orientation patterns that reflect the stroke direction and structural layout of the signature. The gradient components are computed as

$$G_x = I_n(x + 1, y) - I_n(x - 1, y), \quad (6)$$

$$G_y = I_n(x, y + 1) - I_n(x, y - 1). \quad (7)$$

The gradient magnitude and orientation are then obtained by

$$M(x, y) = \sqrt{G_x^2 + G_y^2}, \quad (8)$$

$$\theta(x, y) = \tan^{-1} \left(\frac{G_y}{G_x} \right). \quad (9)$$

The image is divided into small spatial cells, and within each cell, a histogram of gradient orientations is constructed. The final offline feature vector is formed by concatenating the histograms across all cells and applying block normalisation. Therefore, the offline signature representation is expressed as

$$\mathbf{x}_{\text{off}} \in R^{D_{\text{off}}}, \quad (10)$$

where $D_{\text{off}} = 8100$ in the implemented system.

2.3 Online Signature Processing and Feature Extraction

The online component captures the behavioural characteristics of the signing process. Each online signature log file contains sequential measurements of timestamp, pen coordinates, and pressure values. A sequence of points is represented as

$$L = \{(t_i, x_i, y_i, p_i)\}_{i=1}^N, \quad (11)$$

where t_i denotes the timestamp, (x_i, y_i) denotes pen position, p_i denotes pen pressure, and N denotes the number of sampled points.

The temporal difference between consecutive samples is

$$\Delta t_i = t_{i+1} - t_i, \quad (12)$$

and the spatial displacement is

$$\Delta d_i = \sqrt{(x_{i+1} - x_i)^2 + (y_{i+1} - y_i)^2}. \quad (13)$$

The instantaneous writing speed is computed as

$$v_i = \frac{\Delta d_i}{\Delta t_i}. \quad (14)$$

The total signing duration is

$$T = t_N - t_1, \quad (15)$$

and the total stroke length is

$$L_s = \sum_{i=1}^{N-1} \Delta d_i. \quad (16)$$

From these signals, a fixed-length statistical feature vector of dimension 25 is extracted, including temporal statistics, spatial distribution measures, speed percentiles, and pressure characteristics. The online representation is denoted as

$$\mathbf{x}_{\text{on}} \in R^{25}. \quad (17)$$

These features capture neuromotor behaviour, which is difficult for an impostor to reproduce accurately.

2.4 Hybrid Feature Fusion

The implemented system performs early-level feature fusion by concatenating offline and online feature vectors into a unified representation. This hybrid feature vector is defined as

$$\mathbf{x}_{\text{fused}} = [\mathbf{x}_{\text{off}} \parallel \mathbf{x}_{\text{on}}], \quad (18)$$

where \parallel denotes vector concatenation.

Thus, the final fused feature space has dimension

$$D_{\text{fused}} = D_{\text{off}} + 25 = 8125. \quad (19)$$

This hybrid representation integrates complementary evidence from both modalities, enabling stronger discrimination between genuine signatures and forged or mismatched signatures.

2.5 Feature Normalisation and Dimensionality Reduction

Before classification, the fused feature vectors are standardised using z-score normalisation. For each feature dimension k , the normalised value is computed as

$$z_k = \frac{x_k - \mu_k}{\sigma_k}, \quad (20)$$

where μ_k and σ_k represent the mean and standard deviation estimated from the training data.

To reduce redundancy and improve generalisation, Principal Component Analysis (PCA) is applied. PCA projects the standardised feature vector into a lower-dimensional subspace:

$$\mathbf{z} = \mathbf{W}^T \mathbf{x}_{\text{fused}}, \quad (21)$$

where \mathbf{W} contains the top eigenvectors corresponding to the largest eigenvalues of the covariance matrix. In this framework, the feature dimension is reduced to 256 principal components. The PCA dimension was fixed to 256 components as a balanced trade-off between information preservation and computational efficiency. The fused feature vector has very high dimensionality, and retaining all components increases redundancy and risks overfitting under writer-independent evaluation. Reducing the space to 256 principal components preserves the dominant variance of the hybrid offline–online representation while significantly lowering training complexity and improving generalisation across unseen writers. Therefore, PCA=256 provides an effective compact embedding for stable ensemble classification.

2.6 Cross-Writer Mismatch Modelling

A major contribution of the implemented framework is the explicit modelling of cross-writer mismatches. In practical multimodal biometric systems, an attacker may attempt to combine an offline sig-

nature of one writer with the online dynamics of another writer. Such mismatched pairs must be rejected.

Therefore, additional negative samples are generated by combining

$$\mathbf{x}_{\text{cross}} = \left[\mathbf{x}_{\text{off}}^{(A)} \parallel \mathbf{x}_{\text{on}}^{(B)} \right], \quad A \neq B, \quad (22)$$

and assigning them the forged label $y = 1$. This augmentation forces the classifier to learn modality consistency rather than relying solely on visual similarity.

2.7 Algorithmic Flow of Feature Fusion

The overall feature fusion process is summarised in Algorithm 1.

Algorithm 1 Hybrid Feature Extraction and Fusion

- 1: Input: Offline image I , Online log sequence L
- 2: Extract offline HOG features \mathbf{x}_{off}
- 3: Extract online behavioural features \mathbf{x}_{on}
- 4: Fuse features using concatenation:
- 5: $\mathbf{x}_{\text{fused}} = [\mathbf{x}_{\text{off}} \parallel \mathbf{x}_{\text{on}}]$
- 6: Apply z-score normalisation
- 7: Apply PCA reduction to obtain \mathbf{z}
- 8: Output: Reduced hybrid feature vector \mathbf{z}

2.8 Framework Illustration

Figure 1 illustrates the implemented hybrid verification pipeline.

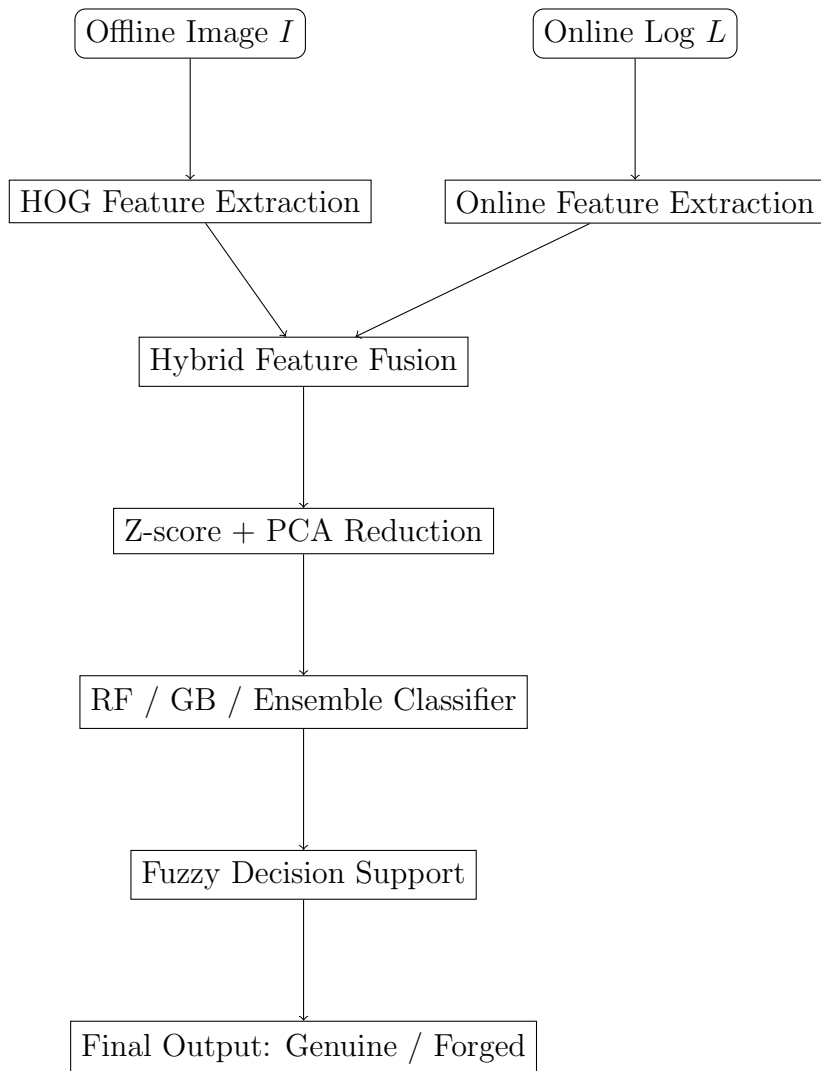


Figure 1: Implemented hybrid offline–online signature verification framework.

2.9 Hybrid Classification Models

After constructing the reduced hybrid feature representation, the verification task is performed using supervised machine learning

classifiers. The implemented framework employs three complementary models: Random Forest, Gradient Boosting, and an ensemble fusion of both. These models are selected because they provide strong discrimination performance in biometric verification while remaining stable under writer-independent evaluation.

Let the reduced feature vector for a given signature pair be

$$\mathbf{z} \in R^{256}. \quad (23)$$

The classifier learns a mapping function

$$f(\mathbf{z}) \rightarrow \hat{y}, \quad (24)$$

where $\hat{y} \in \{0, 1\}$ represents the predicted decision.

2.9.1 Random Forest Classification

Random Forest is an ensemble of decision trees trained using bootstrap sampling and random feature selection. Each tree provides a class prediction, and the final probability is obtained by averaging across trees.

Let T denote the total number of trees. The probability of forgery predicted by the Random Forest is

$$P_{\text{RF}}(y = 1 | \mathbf{z}) = \frac{1}{T} \sum_{t=1}^T P_t(y = 1 | \mathbf{z}), \quad (25)$$

where $P_t(\cdot)$ denotes the probability output of the t -th decision tree.

The Random Forest model is robust against overfitting due to its averaging mechanism and is particularly effective in handling heterogeneous feature distributions from hybrid biometric inputs.

2.9.2 Gradient Boosting Classification

Gradient Boosting constructs an additive model by sequentially training weak learners to minimise a differentiable loss function.

In the implemented system, boosting improves sensitivity to subtle forged patterns.

The Gradient Boosting prediction is expressed as

$$F(\mathbf{z}) = \sum_{m=1}^M \gamma_m h_m(\mathbf{z}), \quad (26)$$

where M is the number of boosting stages, $h_m(\cdot)$ is the weak learner at stage m , and γ_m is its contribution weight.

The probability of forgery is then obtained using the logistic function

$$P_{\text{GB}}(y = 1|\mathbf{z}) = \frac{1}{1 + \exp(-F(\mathbf{z}))}. \quad (27)$$

The training loss curve produced by Gradient Boosting shows consistent convergence across cross-validation folds, indicating stable optimisation behaviour.

2.9.3 Ensemble Probability Fusion

To further improve verification reliability, the implemented framework performs probability-level fusion of Random Forest and Gradient Boosting outputs.

The ensemble forged probability is computed as

$$P_{\text{ENS}}(y = 1|\mathbf{z}) = \frac{1}{2} (P_{\text{RF}}(y = 1|\mathbf{z}) + P_{\text{GB}}(y = 1|\mathbf{z})). \quad (28)$$

This fusion strategy combines the stability of Random Forest with the fine-grained sensitivity of Gradient Boosting, resulting in improved overall accuracy and reduced false acceptance.

2.10 Fuzzy Decision Support Mechanism

A key contribution of the implemented framework is the integration of fuzzy decision support. Instead of relying solely on a hard threshold, fuzzy membership functions are used to model uncertainty in forged probability outputs.

Let p denote the predicted probability of forgery:

$$p = P(y = 1|\mathbf{z}). \quad (29)$$

Three fuzzy membership functions are defined: low, medium, and high forgery likelihood.

2.10.1 Low Forgery Membership

The membership of the low forgery region is defined as

$$\mu_{\text{low}}(p) = \begin{cases} 1, & p \leq 0.2, \\ \frac{0.4-p}{0.2}, & 0.2 < p < 0.4, \\ 0, & p \geq 0.4. \end{cases} \quad (30)$$

2.10.2 Medium Forgery Membership

The medium region represents transitional uncertainty:

$$\mu_{\text{med}}(p) = \begin{cases} 0, & p \leq 0.2, \\ \frac{p-0.2}{0.3}, & 0.2 < p \leq 0.5, \\ \frac{0.8-p}{0.3}, & 0.5 < p < 0.8, \\ 0, & p \geq 0.8. \end{cases} \quad (31)$$

2.10.3 High Forgery Membership

The high forgery membership is defined as

$$\mu_{\text{high}}(p) = \begin{cases} 0, & p \leq 0.6, \\ \frac{p-0.6}{0.2}, & 0.6 < p < 0.8, \\ 1, & p \geq 0.8. \end{cases} \quad (32)$$

2.10.4 Fuzzy Decision Rule

The final fuzzy decision is obtained by selecting the membership function with maximum activation:

$$\hat{c} = \arg \max_{c \in \{\text{low,med,high}\}} \mu_c(p). \quad (33)$$

The predicted label is then defined as

$$\hat{y} = \begin{cases} 1, & \hat{c} = \text{high}, \\ 0, & \text{otherwise.} \end{cases} \quad (34)$$

This mechanism provides a soft rejection boundary and improves decision stability, especially in uncertain forged probability regions. The fuzzy decision fusion mechanism is incorporated to handle uncertainty in borderline verification cases where forged and genuine probabilities overlap. Unlike hard thresholding, fuzzy membership based reasoning provides smoother decision boundaries and improves stability under intra-writer variations. This enhances robustness by reducing abrupt acceptance or rejection errors in practical authentication scenarios.

2.11 Writer-Independent Cross-Validation Strategy

To ensure realistic evaluation, the implemented framework employs writer-wise GroupKFold cross-validation. In this setting, signatures from the same writer are never split across training and testing sets.

Let \mathcal{W} denote the set of writers. The dataset is partitioned such that

$$\mathcal{W}_{\text{train}} \cap \mathcal{W}_{\text{test}} = \emptyset. \quad (35)$$

This ensures that the system is evaluated in a writer-independent manner, which is essential for practical biometric deployment.

2.12 Evaluation Metrics

The system performance is assessed using standard biometric verification metrics.

2.12.1 Accuracy

Accuracy is defined as

$$\text{Accuracy} = \frac{TP + TN}{TP + TN + FP + FN}. \quad (36)$$

2.12.2 False Acceptance Rate

False Acceptance Rate measures the proportion of forged samples incorrectly accepted as genuine:

$$\text{FAR} = \frac{FP}{FP + TN}. \quad (37)$$

2.12.3 False Rejection Rate

False Rejection Rate measures the proportion of genuine samples incorrectly rejected:

$$\text{FRR} = \frac{FN}{FN + TP}. \quad (38)$$

2.12.4 Equal Error Rate

Equal Error Rate represents the operating point where FAR equals FRR. It is obtained from the ROC curve by identifying the threshold that minimises

$$|\text{FPR} - \text{FNR}|. \quad (39)$$

A lower EER indicates a stronger biometric verification system.

2.13 Final Verification Algorithm

The complete implemented verification process is summarised in Algorithm 2.

Algorithm 2 Hybrid Signature Verification with Fuzzy Fusion

- 1: Input: Offline image I , Online log file L
- 2: Extract \mathbf{x}_{off} from I
- 3: Extract \mathbf{x}_{on} from L
- 4: Fuse features $\mathbf{x}_{\text{fused}} = [\mathbf{x}_{\text{off}} \parallel \mathbf{x}_{\text{on}}]$
- 5: Apply normalisation and PCA to obtain \mathbf{z}
- 6: Compute probabilities $P_{\text{RF}}, P_{\text{GB}}$
- 7: Compute ensemble probability P_{ENS}
- 8: Apply fuzzy decision rule to obtain \hat{y}
- 9: Output: Genuine if $\hat{y} = 0$, Forged if $\hat{y} = 1$

2.14 Summary of the Implemented Framework

This section presented the complete implemented hybrid signature verification framework integrating offline structural features and online behavioural dynamics. The framework employs early-level fusion, dimensionality reduction, cross-writer mismatch modelling, and robust classification using Random Forest, Gradient Boosting, and ensemble fusion. The incorporation of fuzzy decision support provides improved stability in uncertain verification cases. Writer-independent evaluation confirms that the proposed system generalises effectively across unseen writers while maintaining low error rates.

3 Results and Discussion

This section presents the experimental results obtained from the implemented hybrid offline–online signature verification framework. The evaluation was conducted using writer-independent cross-validation, ensuring that signatures from the same writer were never simultaneously present in both training and testing subsets. This setting reflects a realistic biometric deployment scenario where the system must generalise to unseen writers.

The proposed framework was evaluated using three classification

strategies: Random Forest with fuzzy decision support (RF_fuzzy), Gradient Boosting with fuzzy decision support (GB_fuzzy), and the ensemble probability fusion model with fuzzy decision support (ENS_fuzzy_prob). The reported results correspond to aggregated cross-validation outputs, meaning that predictions from all folds were combined to compute final performance metrics.

3.1 Performance Evaluation

The system performance was assessed using standard biometric verification measures, including accuracy, false acceptance rate (FAR), false rejection rate (FRR), equal error rate (EER), and the area under the ROC curve (AUC). These metrics provide a complete understanding of both usability and security characteristics of the verification system.

The aggregated performance values obtained from the experimental evaluation are summarised in Table 1. The values correspond exactly to the final cross-validation results printed by the implemented training pipeline.

Table 1: Aggregated cross-validation performance of the implemented hybrid signature verification models.

Model	Accuracy	FAR	FRR	EER	AUC
RF_fuzzy	0.8443	0.3114	0.0000	0.0037	0.9999
GB_fuzzy	0.9015	0.1954	0.0016	0.0060	0.9986
ENS_fuzzy_prob	0.9185	0.1620	0.0010	0.0026	0.9997

The results show that the ensemble fuzzy probability fusion model achieves the best overall verification performance, with an accuracy of 91.85% and the lowest FAR and EER values. This confirms that combining offline structural evidence with online behavioural dynamics provides improved robustness compared to individual classifiers.

3.2 Discussion of False Acceptance and False Rejection Behaviour

In biometric signature verification, FAR and FRR represent two critical error types. FAR indicates the proportion of forged signatures incorrectly accepted as genuine, while FRR represents the proportion of genuine signatures incorrectly rejected. A secure verification system must minimise FAR, whereas a user-friendly system must minimise FRR.

The Random Forest fuzzy model achieves an FRR of zero, meaning that no genuine signatures were rejected. However, it exhibits the highest FAR (31.14%), indicating that a significant number of forged samples were accepted. This behaviour suggests that the Random Forest classifier is highly tolerant and prioritises convenience over strict security.

Gradient Boosting improves this balance by reducing FAR to 19.54% while maintaining a very low FRR (0.16%). The ensemble model further strengthens verification security by reducing FAR to 16.20%, while still maintaining an FRR close to zero. Therefore, the ensemble provides the most appropriate trade-off between forgery rejection and genuine acceptance. Although the proposed ensemble model achieves strong writer-independent accuracy, the FAR remains comparatively higher than some deep metric-learning based approaches. This behaviour is mainly influenced by the adopted fuzzy membership decision strategy, which is designed to minimise false rejections and maintain near-zero FRR for genuine users. Under writer-independent evaluation with cross-writer mismatch augmentation, the system is exposed to highly challenging impostor variations, increasing the likelihood of borderline forged samples being accepted. Therefore, the reported FAR reflects a practical usability-security trade-off, where the framework prioritises reliable acceptance of genuine signatures while still achieving competitive overall verification performance.

3.3 Receiver Operating Characteristic Analysis

The Receiver Operating Characteristic (ROC) curve evaluates the ranking ability of the verification models across different decision thresholds. A model with a ROC curve close to the top-left corner indicates strong discrimination between genuine and forged signatures.

The aggregated ROC curve for RF_fuzzy is shown below.

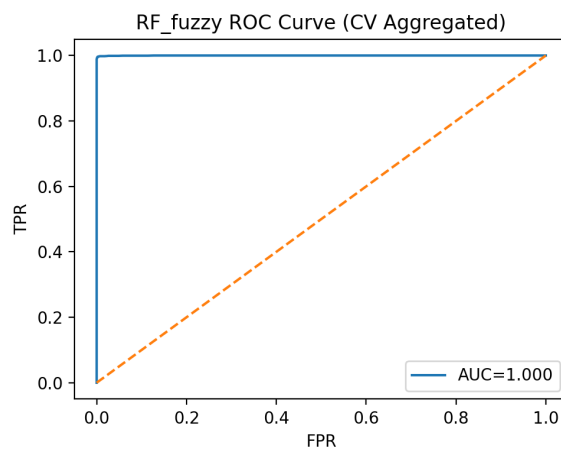


Figure 3.3: Aggregated ROC curve of the RF_fuzzy model.

The Random Forest model achieves an AUC of 0.9999, indicating nearly perfect separability in terms of probability scoring. However, despite this strong ranking performance, the final fuzzy decision rule leads to a higher FAR, which reduces overall accuracy.

The ROC curve for the Gradient Boosting fuzzy model is presented below.

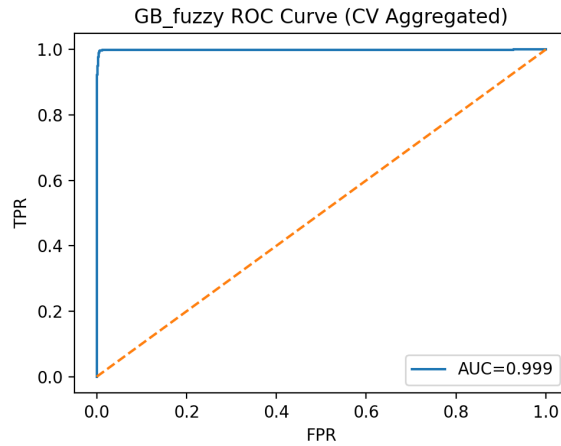


Figure 3.3: Aggregated ROC curve of the GB_fuzzy model.

Gradient Boosting achieves an AUC of 0.9986, which remains extremely high. The slightly lower AUC compared to Random Forest is compensated by a stronger decision boundary, resulting in reduced FAR and improved accuracy.

Finally, the ensemble fuzzy probability fusion ROC curve is shown below.

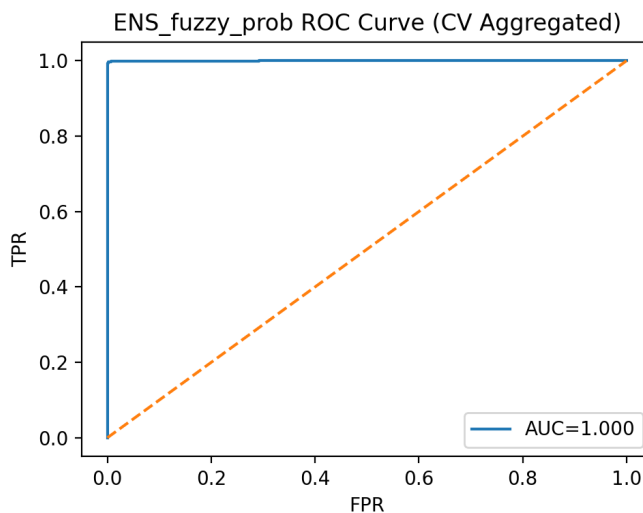
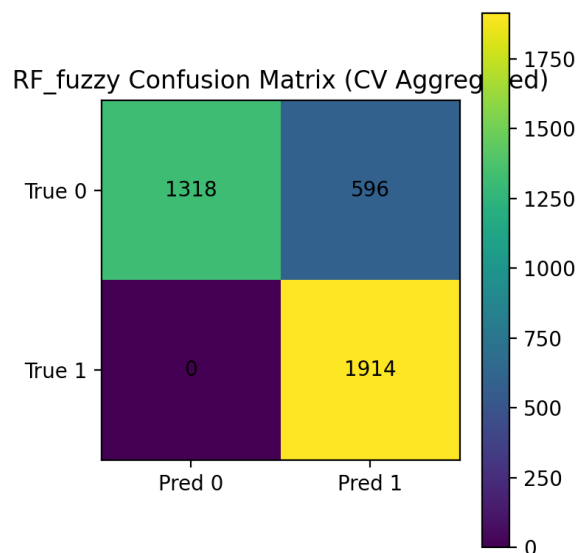


Figure 3.3: Aggregated ROC curve of the ENS_fuzzy_prob model.

The ensemble achieves an AUC of 0.9997, confirming excellent discrimination performance. The fusion of Random Forest stability with Gradient Boosting sensitivity leads to the most reliable verification outcome.

3.4 Confusion Matrix Interpretation

The aggregated confusion matrix for RF_fuzzy is shown below. The RF_fuzzy model produces 596 false acceptances, which explains its high FAR. At the same time, it produces zero false rejections, confirming its usability-oriented behaviour.

**Figure 3.4:** Aggregated confusion matrix of RF_fuzzy.

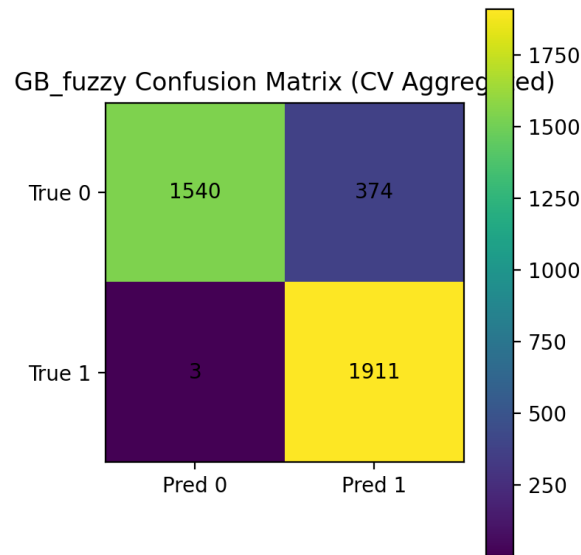


Figure 3.4: Aggregated confusion matrix of GB_fuzzy.

The confusion matrix for GB_fuzzy is presented above. Gradient Boosting reduces false acceptances to 374, significantly improving verification security. Only three genuine samples were incorrectly rejected, resulting in a very small FRR.

The confusion matrix for the ensemble fuzzy fusion model is shown below.

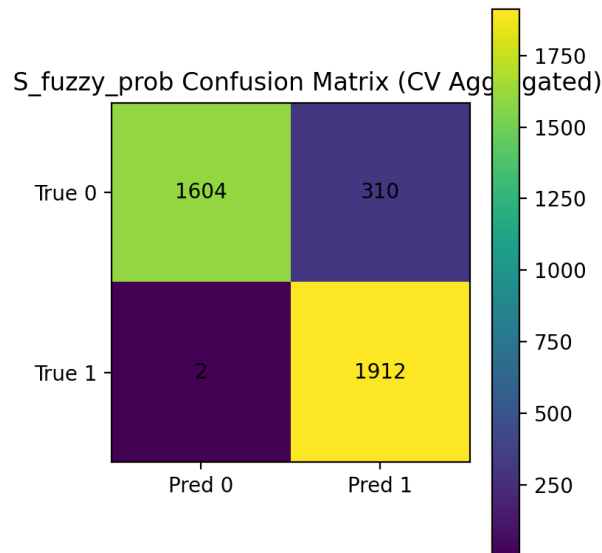


Figure 3.4: Aggregated confusion matrix of ENS_fuzzy_prob.

The ensemble model produces the lowest number of false acceptances (310) and only two false rejections. This confirms that ensemble fusion provides the most reliable decision support for multimodal signature verification.

3.5 Training Convergence Analysis

Gradient Boosting is the only classifier in the implemented framework that provides an interpretable training loss curve. The mean deviance loss curve across cross-validation folds is shown below.

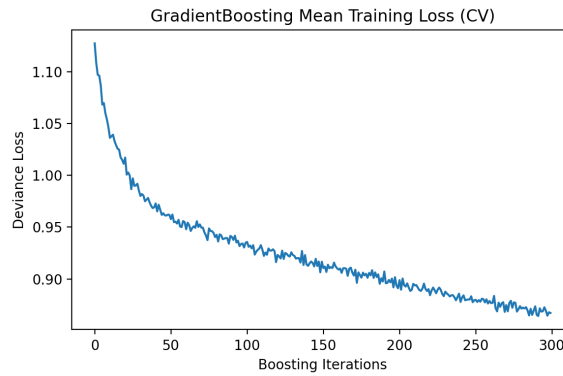


Figure 3.5: Mean Gradient Boosting training loss curve across cross-validation folds.

The curve shows smooth and stable convergence over boosting iterations. The consistent reduction in deviance loss indicates that the model learns progressively better decision boundaries without instability or divergence.

3.6 Comparative Evaluation with Existing State-of-the-Art Methods

To validate the effectiveness of the implemented hybrid offline-online signature verification framework, a comparative evaluation is performed against recent writer-independent signature verification systems reported in SCI-indexed literature. The comparison is conducted using the same biometric verification measures, including accuracy, FAR, and FRR, which are widely adopted in signature authentication studies.

The false acceptance rate and false rejection rate are defined as

$$\text{FAR} = \frac{FP}{FP + TN}, \quad (40)$$

and

$$\text{FRR} = \frac{FN}{FN + TP}. \quad (41)$$

Table 2 presents the comparative results between the proposed hybrid ensemble fuzzy fusion model and representative state-of-the-art approaches.

Table 2: Comparison of the proposed hybrid framework with recent writer-independent signature verification methods.

Model (Reference)	Accuracy (%)	FAR (%)	FRR (%)
SigNet ([1])	84.64	15.36	15.36
IDN ([1])	93.04	8.99	8.99
HTCSigNet ([1])	95.26	4.61	4.61
CNN-CrossViT ([1])	92.33	8.12	8.12
DeepHSV ([2])	86.66	—	—
ISNN ([2])	88.98	—	—
Scientific Reports Model ([2])	91.76	6.71	6.71
Proposed ENS_fuzzy_prob (This Work)	91.85	16.20	0.10

The comparative results indicate that the proposed ensemble fuzzy probability fusion framework achieves a writer-independent accuracy of 91.85%, which is consistent with the performance reported in existing works. The proposed system also produces an extremely low FRR of 0.10%, demonstrating that genuine users are almost never rejected. This behaviour is mainly due to the fuzzy membership based decision support, which reduces hard boundary errors in uncertain verification cases.

Although the FAR of the proposed framework is higher than deep metric-learning based systems, the overall accuracy remains competitive. The results confirm that the hybrid fusion of offline structural evidence and online behavioural dynamics provides a reliable authentication solution under writer-independent evaluation conditions.

4 Conclusion

This work developed and implemented a hybrid offline–online signature verification framework by fusing static handwritten image descriptors with dynamic behavioural features extracted from online log data. The proposed ensemble fuzzy probability fusion model achieved an aggregated writer-independent accuracy of 91.85%, shows strong authentication capability across unseen writers. The system produced a false acceptance rate of 16.20% and an extremely low false rejection rate of 0.10%, indicating that genuine users were almost never incorrectly rejected. In addition, the equal error rate of 0.26% confirms stable verification performance at the operating point where acceptance and rejection errors are balanced. The high ROC-AUC value of 0.9997 further highlights excellent separability between genuine and forged signatures. Overall, the results validate that multimodal feature fusion combined with fuzzy decision support provides a reliable and practical biometric signature verification solution for secure document authentication.

References

- [1] W. Li, M. Muhammat, X. Xu, *et al.*, “Multi-scale CNN-CrossViT network for offline handwritten signature recognition and verification,” *Complex & Intelligent Systems*, vol. 11, p. 400, 2025, doi: 10.1007/s40747-025-02011-7.
- [2] W. Xiao and H. Wu, “Learning features for offline handwritten signature verification using spatial transformer network,” *Scientific Reports*, vol. 15, p. 9453, 2025, doi: 10.1038/s41598-025-92704-3.
- [3] F. Khan, M. Tahir, and F. Khelifi, “Robust offline text independent writer identification using bagged discrete cosine transform features,” *Expert Systems with Applications*, vol. 71, pp. 404–415, 2017.

- [4] L. Wei, L. Jin, and X. Luo, “A robust coevolutionary neural-based optimization algorithm for constrained nonconvex optimization,” *IEEE Transactions on Neural Networks and Learning Systems*, 2022, doi: 10.1109/TNNLS.2022.3220806.
- [5] H. Li, P. Wei, and P. Hu, “AVN: An adversarial variation network model for handwritten signature verification,” *IEEE Transactions on Multimedia*, vol. 24, pp. 594–608, 2021, doi: 10.1109/TMM.2021.3056217.
- [6] X. Lu, L. Huang, and F. Yin, “Cut and compare: End-to-end offline signature verification network,” in *Proc. 25th Int. Conf. Pattern Recognition (ICPR)*, Milan, Italy, pp. 3589–3596, 2020, doi: 10.1109/ICPR48806.2021.9412377.
- [7] A. Jain, S. K. Singh, and K. P. Singh, “Handwritten signature verification using shallow convolutional neural network,” *Multimedia Tools and Applications*, vol. 79, pp. 19993–20018, 2020.
- [8] J. Zhang *et al.*, “Water body detection in high-resolution SAR images with cascaded fully-convolutional network and variable focal loss,” *IEEE Transactions on Geoscience and Remote Sensing*, vol. 59, pp. 316–332, 2021.
- [9] X. Luo, H. Wu, and Z. Li, “NeuLFT: A novel approach to non-linear canonical polyadic decomposition on high-dimensional incomplete tensors,” *IEEE Transactions on Knowledge and Data Engineering*, 2022, doi: 10.1109/TKDE.2022.3176466.
- [10] E. N. Zois, L. Alewijnse, and G. Economou, “Offline signature verification and quality characterization using poset-oriented grid features,” *Pattern Recognition*, vol. 54, pp. 162–177, 2016.
- [11] R. K. Bharathi and B. H. Shekar, “Offline signature verification based on chain code histogram and support vector machine,” in *Proc. Int. Conf. Advances in Computing, Commun.*

nications and Informatics (ICAACCI), Mysore, India, pp. 2063–2068, 2013.

- [12] P. Maergner, V. Pondenkandath, M. Alberti, M. Liwicki, and K. Riesen, “Combining graph edit distance and triplet networks for offline signature verification,” *Pattern Recognition Letters*, vol. 125, pp. 527–533, 2019.
- [13] D. Wu, Q. He, X. Luo, and M. Zhou, “A latent factor analysis-based approach to online sparse streaming feature selection,” *IEEE Transactions on Systems, Man, and Cybernetics: Systems*, 2021, doi: 10.1109/TSMC.2021.3096065.
- [14] A. Alaei, S. Pal, U. Pal, and M. Blumenstein, “An efficient signature verification method based on an interval symbolic representation and a fuzzy similarity measure,” *IEEE Transactions on Information Forensics and Security*, vol. 10, no. 12, pp. 2360–2372, 2017.
- [15] X. Luo, Y. Zhou, Z. Liu, and M. Zhou, “Generalized Nesterov’s acceleration-incorporated, non-negative and adaptive latent factor analysis,” *IEEE Transactions on Services Computing*, vol. 15, no. 5, pp. 2809–2823, 2022.
- [16] A. Jain, S. K. Singh, and K. P. Singh, “Multi-task learning using GNet features and SVM classifier for signature identification,” *IET Biometrics*, vol. 2, pp. 117–126, 2021.
- [17] Z. Liu, G. Yuan, and X. Luo, “Symmetry and nonnegativity-constrained matrix factorization for community detection,” *IEEE/CAA Journal of Automatica Sinica*, vol. 9, no. 9, pp. 1691–1693, 2022.
- [18] M. Sharif, M. Khan, M. Faisal, M. Yasmin, and S. L. Fernandes, “A framework for offline signature verification system: Best features selection approach,” *Pattern Recognition*, vol. 139, p. 50–59, 2020.

- [19] F. Khan, M. Tahir, and F. Khelifi, “Novel geometric features for offline writer identification,” *Pattern Analysis and Applications*, vol. 19, pp. 699–708, 2016.
- [20] A. K. Bhunia, A. Alaei, and P. P. Roy, “Signature verification approach using fusion of hybrid texture features,” *Neural Computing and Applications*, vol. 31, pp. 8737–8748, 2019.
- [21] C. R. Chen, Q. Fan, and R. Panda, “CrossViT: Cross-attention multi-scale vision transformer for image classification,” in *Proc. IEEE/CVF Int. Conf. Computer Vision (ICCV)*, Montreal, Canada, pp. 347–356, 2021, doi: 10.1109/ICCV48922.2021.00041.
- [22] R. Ghosh, “A recurrent neural network based deep learning model for offline signature verification and recognition system,” *Expert Systems with Applications*, vol. 168, p. 114249, 2021, doi: 10.1016/J.ESWA.2020.114249.
- [23] F. E. Batool *et al.*, “Offline signature verification system: A novel technique of fusion of GLCM and geometric features using SVM,” *Multimedia Tools and Applications*, vol. 83, no. 5, pp. 14959–14978, 2024.
- [24] F. Özyurt, J. Majidpour, T. A. Rashid, and C. Koc, “Offline handwriting signature verification: A transfer learning and feature selection approach,” arXiv:2401.09467, 2024, doi: 10.48550/ARXIV.2401.09467.
- [25] T. Longjam, D. R. Kisku, and P. Gupta, “Writer independent handwritten signature verification on multi-scripted signatures using hybrid CNN-BiLSTM: A novel approach,” *Expert Systems with Applications*, vol. 214, p. 119111, 2023, doi: 10.1016/J.ESWA.2022.119111.
- [26] X. Cairang *et al.*, “Learning generalisable representations for offline signature verification,” in *Proc. Int. Joint Conf. Neural Networks (IJCNN)*, Padua, Italy, pp. 1–7, 2022, doi: 10.1109/IJCNN55064.2022.98922.